

Chapter 11

The hovercraft model

11.1 Introduction

Nowadays, control problems of underactuated vehicles motivate the development of new non-linear control design methodologies. Such systems are vehicles with fewer independent control inputs than degrees of freedom to be controlled.

In order to capture the essential non-linear behavior of an underactuated ship, we have simplified its model as found in [25]. Neglecting the damping, we have considered that the shape of the ship is symmetric with respect to three axes, mainly a circle and that the two propellers are situated at the center of mass. Therefore, after these simplifications, we obtain the model of a hovercraft that has two propellers to move the vehicle forwards (and backwards) and to make it turn. The main difference with respect to a two-wheel mobile robot is that a hovercraft can move freely sideways, even though this degree of freedom is not actuated. The hovercraft model presented here will be used to design a control strategy and the purpose is to promote the development of new control design methods, such as the studies of other highly non-linear mechanical systems like the ball and beam and the inverted pendulum have done.

A picture of a model kit representing a real hovercraft (the “LCAC-1 Navy Assault Hovercraft”) is shown in Figure 11.1. The Landing Craft Air Cushion (LCAC-1) is an assault vehicle designed to transport U.S. Marine fighting forces from naval ships off-shore to inland combat positions. The model kit is a reproduction of the 200 ton craft.

We will first consider the problem of regulating the surge, the sway and the angular velocities to zero. We will also propose strategies for

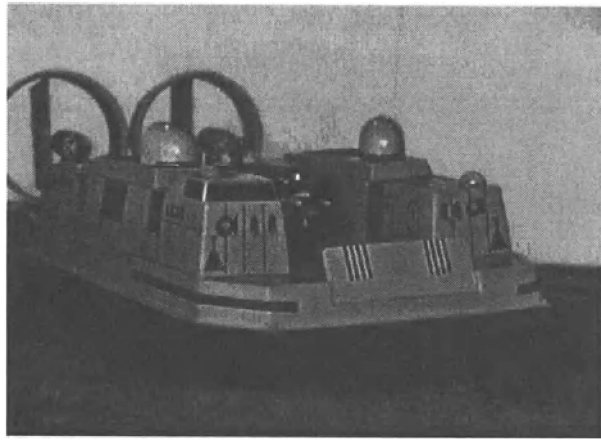


Figure 11.1: LCAC-1 Navy Assault Hovercraft

positioning the hovercraft at the origin.

Various control algorithms for controlling underactuated vessels have appeared in the literature. Leonard [51] was the first to control a dynamic autonomous underwater vessel model (AUV model) with force and torque control inputs. It was shown how open-loop periodic time-varying control can be used to control underwater vehicles. Pettersen and Egeland [82] developed a stability result involving continuous time-varying feedback laws that exponentially stabilize both the position and orientation of a surface vessel having only two control inputs. This result was extended to include integral action in [83]. Other approaches also exist in the literature like the one in Fossen et al. [26], which considered a non-linear ship model including the hydrodynamic effects due to time-varying speed and wave frequency. This involved a non-symmetrical inertia matrix and non-positive damping at high-speed. The authors used a backstepping technique for tracking control design. Bullo and Leonard [15] developed high-level motion procedures that solved point-to-point reconfiguration, local exponential stabilization and static interpolation problems for underactuated vehicles. Strand et al. [112] proposed a stabilizing controller for moored and free-floating (but not underactuated) ships constructed by backstepping. They proposed a locally asymptotically convergent algorithm based on H_∞ -optimal control. They also presented a global result using inverse optimality for the non-linear system. Pettersen and Nijmeijer [85] proposed a time-varying feedback control law that provides global

practical stabilization and tracking, using a combined integrator backstepping and averaging approach. In [84], they proposed a tracking control law that steers both position and course angle of the surface vessel, providing semi-global exponential stabilization of the desired trajectory. Berge et al. [9] developed a tracking controller for the underactuated ship using partial feedback linearization. The control law makes the position and velocities converge exponentially to the reference trajectory, while the course angle of the ship is not controlled.

One of the difficulties encountered in the stabilization of underactuated vehicles is that classical non-linear techniques in non-linear control theory like feedback linearization are not applicable. Therefore, new design methodologies should be explored.

In the present chapter, we propose two different control strategies. The first controller globally and asymptotically stabilizes the surge, sway and angular velocities with a differentiable controller. In this case, we consider the surge force and the angular torque as inputs. In the second controller, we globally and asymptotically stabilizes the position and the sway velocities at the origin using the surge and the angular velocities as inputs. The proposed controller is discontinuous. In both cases, the analysis is based on a Lyapunov approach. This chapter refers to the work [22]. The chapter is organized as follows. In Section 11.2, the model of the simplified ship is recalled. Section 11.3 presents the control algorithm to stop the hovercraft. Section 11.4 is devoted to the control strategy for positioning of the hovercraft. Section 11.5 gives simulation results.

11.2 The hovercraft model

In this section, the mathematical model of the hovercraft system as shown in Figure 11.2 is obtained using both Newton's second law and the Euler-Lagrange formulation.

11.2.1 System model using Newton's second law

We consider the class of underactuated vehicles described by the following general model (see [25])

$$M\dot{\nu} + C(\nu)\nu + D(\nu)\nu + g(\eta) = \begin{bmatrix} \tau \\ 0 \end{bmatrix} \quad (11.1)$$

$$\dot{\eta} = J(\eta)\nu \quad (11.2)$$

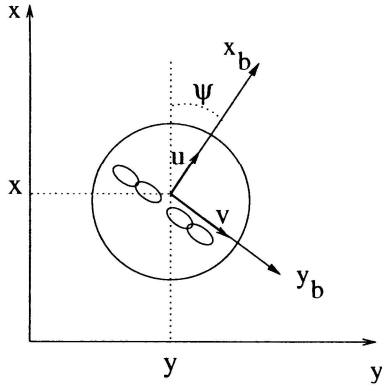


Figure 11.2: The hovercraft

where $\eta \in \mathbb{R}^n$, $\nu \in \mathbb{R}^n$, $\tau \in \mathbb{R}^m$, $m < n$. The matrices M and J are non-singular and $\dot{M} = 0$. This class of systems includes underactuated surface vessels, underwater vehicles, aeroplanes and spacecraft. The vector ν denotes the linear and angular velocities decomposed in the body-fixed frame, η denotes the position and orientation decomposed in the earth-fixed frame, and τ denotes the control forces and torques decomposed in the body-fixed frame. M is the inertia matrix. $C(\nu)$ is the Coriolis and centripetal matrix. $D(\nu)$ is the damping matrix and $g(\eta)$ is the vector of gravitational and possibly buoyant forces and torques. Equations (11.1) and (11.2) represent the dynamics and the kinematics respectively.

Using the previous model (11.1)-(11.2), a surface vessel having two independent main propellers is described by the following model (see [81])

$$\begin{bmatrix} m_{11} & 0 & 0 \\ 0 & m_{22} & m_{23} \\ 0 & m_{23} & m_{33} \end{bmatrix} \begin{bmatrix} \dot{u} \\ \dot{v} \\ \dot{r} \end{bmatrix} + \begin{bmatrix} 0 & 0 & -f(v, r) \\ 0 & 0 & m_{11}u \\ f(v, r) & m_{11}u & 0 \end{bmatrix} \begin{bmatrix} u \\ v \\ r \end{bmatrix} + \begin{bmatrix} -X_u & 0 & 0 \\ 0 & -Y_u & -Y_r \\ 0 & -N_v & -N_r \end{bmatrix} \begin{bmatrix} u \\ v \\ r \end{bmatrix} = \begin{bmatrix} \tau_u \\ 0 \\ \tau_r \end{bmatrix} \quad (11.3)$$

$$\begin{bmatrix} \dot{x} \\ \dot{y} \\ \dot{\psi} \end{bmatrix} = \begin{bmatrix} \cos(\psi) & -\sin(\psi) & 0 \\ \sin(\psi) & \cos(\psi) & 0 \\ 0 & 0 & 1 \end{bmatrix} \begin{bmatrix} u \\ v \\ r \end{bmatrix} \quad (11.4)$$

where $f(v, r) = m_{23}r + m_{22}v$. The matrices are denoted M , $C(\nu)$,

D and $J(\eta)$ according to (11.1)-(11.2). M and D are both constant, positive definite matrices. The vector $\nu = [u, v, r]^T$ denotes the linear velocities in surge, sway and the angular velocity in yaw respectively. $\eta = [x, y, \psi]^T$ is the position and orientation vector and $\tau = [\tau_u, 0, \tau_r]^T$ denotes the control forces in surge and the control torque in yaw respectively.

The non-linear model for an underactuated hovercraft is obtained by simplifying the surface vessel model presented above (see [85] and [84]). We have neglected damping, considered that the shape of the hovercraft is a disc and that the propellers are located at the center of mass as shown in Figure 11.2. In order to obtain a simple model capturing the essential non-linearities of a hovercraft, we assumed the inertia matrix in (11.3) to be diagonal and equal to the identity matrix. Moreover, we cancelled the hydrodynamic damping, which is not essential in controlling the system. The dynamic equations are then given by (see [82])

$$\begin{aligned}\dot{u} &= vr + \tau_u \\ \dot{v} &= -ur \\ \dot{r} &= \tau_r\end{aligned}\tag{11.5}$$

where τ_u is the control force in surge and τ_r is the control torque in yaw. In the second equation of system (11.5), the right term represents Coriolis and centripetal forces.

11.2.2 Euler-Lagrange's equations

Using the same assumptions as the previous section, the Lagrangian function for the system described in Figure 11.2 is given by

$$L = \frac{1}{2}\dot{x}^2 + \frac{1}{2}\dot{y}^2 + \frac{1}{2}\dot{\psi}^2\tag{11.6}$$

The corresponding equations of motion are derived using Lagrange's equations

$$\frac{d}{dt} \left(\frac{\partial L}{\partial \dot{q}} (q, \dot{q}) \right) - \frac{\partial L}{\partial q} (q, \dot{q}) = \tau\tag{11.7}$$

where $q = [x, y, \psi]^T$ and $\tau = [\tau_u \cos(\psi), \tau_u \sin(\psi), \tau_r]^T$. From La-grange's equations (11.7), we therefore have

$$\begin{aligned}\ddot{x} &= \tau_u \cos(\psi) \\ \ddot{y} &= \tau_u \sin(\psi) \\ \ddot{\psi} &= \tau_r\end{aligned}$$

Let us recall the kinematics (11.4) as follows

$$\begin{aligned}\dot{x} &= \cos(\psi)u - \sin(\psi)v \\ \dot{y} &= \sin(\psi)u + \cos(\psi)v \\ \dot{\psi} &= r\end{aligned}\tag{11.8}$$

Differentiating the above equations (11.8), we obtain

$$\ddot{x} = -\sin(\psi)ru + \cos(\psi)\dot{u} - \cos(\psi)rv - \sin(\psi)\dot{v}\tag{11.9}$$

$$\ddot{y} = \cos(\psi)ru + \sin(\psi)\dot{u} - \sin(\psi)rv + \cos(\psi)\dot{v}\tag{11.10}$$

$$\ddot{\psi} = \tau_r$$

Multiplying (11.9) by $\cos(\psi)$ and (11.10) by $\sin(\psi)$ and adding these two equations yields

$$\begin{aligned}\dot{u} &= \cos(\psi)\ddot{x} + \sin(\psi)\ddot{y} + vr \\ \dot{u} &= \tau_u + vr\end{aligned}\tag{11.11}$$

Multiplying (11.9) by $\sin(\psi)$ and (11.10) by $\cos(\psi)$ and adding these two equations yields

$$\begin{aligned}\dot{v} &= \cos(\psi)\ddot{y} - \sin(\psi)\ddot{x} - ur \\ \dot{v} &= -ur\end{aligned}\tag{11.12}$$

We finally obtain the dynamic equations (11.5)

$$\begin{aligned}\dot{u} &= \tau_u + vr \\ \dot{v} &= -ur \\ \dot{r} &= \tau_r\end{aligned}\tag{11.13}$$

We will, in the following, consider the problem of controlling the position, not the yaw angle ψ and thus disregard the latter equation in (11.8). In order to achieve simpler polynomial kinematic equations and

to eliminate ψ , we use the following coordinate transformation as in [82], which is a global diffeomorphism

$$\begin{aligned} z_1 &= \cos(\psi)x + \sin(\psi)y \\ z_2 &= -\sin(\psi)x + \cos(\psi)y \\ z_3 &= \psi \end{aligned} \quad (11.14)$$

Differentiating z_1 and z_2 and using (11.8), we obtain

$$\begin{aligned} \dot{z}_1 &= u + z_2 r \\ \dot{z}_2 &= v - z_1 r \end{aligned} \quad (11.15)$$

The resulting model, including the kinematics and the dynamics, is finally given by

$$\begin{aligned} \dot{u} &= vr + \tau_u \\ \dot{v} &= -ur \\ \dot{r} &= \tau_r \\ \dot{z}_1 &= u + z_2 r \\ \dot{z}_2 &= v - z_1 r \end{aligned} \quad (11.16)$$

11.2.3 Controllability of the linearized system

Since the third equation ($\dot{r} = \tau_r$) in (11.16) is directly controllable, let us consider the linearization of the four other equations.

The system can be rewritten as follows

$$\frac{d}{dt} \begin{bmatrix} u \\ v \\ z_1 \\ z_2 \end{bmatrix} = \begin{bmatrix} 0 & r & 0 & 0 \\ -r & 0 & 0 & 0 \\ 1 & 0 & 0 & r \\ 0 & 1 & -r & 0 \end{bmatrix} \begin{bmatrix} u \\ v \\ z_1 \\ z_2 \end{bmatrix} + \begin{bmatrix} 1 \\ 0 \\ 0 \\ 0 \end{bmatrix} \tau_u = AX + B\tau_u$$

We then have

$$B = \begin{bmatrix} 1 \\ 0 \\ 0 \\ 0 \end{bmatrix} \quad AB = \begin{bmatrix} 0 \\ -r \\ 1 \\ 0 \end{bmatrix} \quad A^2B = \begin{bmatrix} -r^2 \\ 0 \\ 0 \\ -2r \end{bmatrix} \quad A^3B = \begin{bmatrix} 0 \\ r^3 \\ -3r^2 \\ 0 \end{bmatrix}$$

and $\det(B|AB|A^2B|A^3B) = 4r^4$.

Therefore, the linearized system is controllable if $r \neq 0$. A very simple control strategy can be obtained by fixing r to a constant different from zero and computing a linear controller for the input τ_u . This controller will exponentially stabilize (u, v, z_1, z_2) to the origin but r will not converge to zero.

Furthermore, if r is time-varying, we could use the Silverman's criterion to check the controllability of the system, i.e.

$$\text{rank } C(t) = \left[b(t), (A(t) - \frac{d}{dt})b(t), \dots, (A(t) - \frac{d}{dt})^{n-1}b(t) \right] = 4 \quad (11.17)$$

In our case, $\det(C(t)) = 4r^4$. Therefore, if r is time-varying, the system is controllable at all time if $r(t) \neq 0, \forall t$.

11.3 Stabilizing control law for the velocity

The dynamics of the system are given as follows

$$\begin{aligned} \dot{u} &= vr + \tau_u \\ \dot{v} &= -ur \\ \dot{r} &= \tau_r \end{aligned} \quad (11.18)$$

The objective is to stop the hovercraft, i.e. to control “the state vector $[u \ v \ r]^T$ ” with the two inputs “ τ_u and τ_r ”. τ_u and τ_r are the surge control force and the yaw control torque provided by the main propellers.

We propose the control law

$$\tau_u = -k_u u \quad (11.19)$$

$$\tau_r = -ur - k_r(r - v) \quad (11.20)$$

where k_u and k_r are strictly positive constants. Consider the candidate Lyapunov function

$$V_1(u, v, r) = \frac{1}{2}u^2 + \frac{1}{2}v^2 + \frac{1}{2}(r - r_d)^2 \quad (11.21)$$

with $r_d = v$. The time derivative of V_1 is then

$$\begin{aligned} \dot{V}_1 &= u(vr + \tau_u) - uvr + (r - v)(\tau_r + ur) \\ &= -k_u u^2 - k_r(r - v)^2 \end{aligned}$$

Using LaSalle's invariance principle, we consider the set $\Omega = \{(u, v, r) : \dot{V}_1(u, v, r) = 0\} = \{(u, v, r) : u = 0, r = v\}$. From (11.19), we see that $\tau_u = 0$ in Ω and from (11.18) this implies $r = v$ has to be zero to stay in Ω . Thus Ω contains no trajectory of (11.18) other than the trivial trajectory, and the continuous control law in (11.19) and (11.20) globally and asymptotically stabilizes the origin of the state $[u \ v \ r]^T$.

11.4 Stabilization of the position

11.4.1 First approach

In this section, we will develop a control law for positioning the hovercraft using the surge and angular velocities u and r as virtual control inputs. The model in (11.16) reduces to

$$\begin{aligned}\dot{z}_1 &= u + z_2 r \\ \dot{z}_2 &= v - z_1 r \\ \dot{v} &= -ur\end{aligned}\tag{11.22}$$

Note that the above system satisfies Brockett's condition while it would not if we have added the equation for the course angle: $\dot{\psi} = r$. Consider the following candidate Lyapunov function

$$V_2 = \frac{1}{2}z_1^2 + \frac{1}{2}z_2^2 + \frac{1}{2}v^2\tag{11.23}$$

Then

$$\dot{V}_2 = z_1 u + z_2 v - u v r = z_1 u + v(z_2 - u r)$$

We propose

$$\begin{cases} ur &= z_2 + v \\ u &= -\text{sign}(z_1)\phi \end{cases}\tag{11.24}$$

where $\text{sign}(0) = 1$ and ϕ is a positive definite function defined by

$$\phi = \left[\frac{1}{2} (z_1^2 + z_2^2 + v^2) \right]^{\frac{1}{4}}\tag{11.25}$$

The resulting control input r is

$$r = \frac{z_2 + v}{-\text{sign}(z_1)\phi} \quad (11.26)$$

Obviously r is a discontinuous function. The time derivative of V_2 is given by

$$\dot{V}_2 = -|z_1|\phi - v^2 \quad (11.27)$$

It follows that \dot{V}_2 is negative and so V_2 converges. Therefore, z_1 , z_2 and v remain bounded. Note that although r in (11.26) is a discontinuous function, r is bounded on any compact set. Integrating (11.27), it follows that $\int_0^t v^2 dt$ and $\int_0^t |z_1|\phi dt$ are finite. From (11.22) and (11.24), it follows that \dot{v} is bounded, which implies that v is uniformly continuous. Using Barbalat's lemma, it follows that $v \rightarrow 0$. Then, since $\dot{z}_2 = v - z_1 r$ is bounded, z_2 is uniformly continuous. From (11.22) and (11.24), we have $\dot{v} = -ur = -z_2 + v$, then \dot{v} is uniformly continuous. It follows that $\dot{v} \rightarrow 0$, using Barbalat's lemma. Using again $\dot{v} = -ur = -z_2 + v$ and $v \rightarrow 0$, it also follows that $z_2 \rightarrow 0$. Since V_2 converges, it follows that z_1 converges to a constant $z_1(\infty)$. We will study two different cases:

- Case a: If $z_1(\infty) = 0$, the state (z_1, z_2, v) converges asymptotically to the origin and the inputs u and r converge to zero.
- Case b: If $z_1(\infty) \neq 0$ then there exists a finite time T such that

$$|z_1| > \frac{1}{2}|z_1(\infty)| \quad \forall t \geq T$$

Therefore

$$\int_T^t |z_1|\phi dt \geq \frac{|z_1(\infty)|}{2} \int_T^t \phi(t) dt$$

Since the left hand side of the above is finite and ϕ is uniformly continuous, it follows from Barbalat's lemma that $\phi \rightarrow 0$.

Finally, we conclude that the state (z_1, z_2, v) and the inputs u and r converge asymptotically to zero.

11.4.2 Second approach

In this section, we present an alternative control scheme for achieving positioning of the hovercraft. The advantage of the control strategy proposed here is that the control inputs are smoother than those of the control proposed in the previous section. We will prove also that the state (z_1, z_2, v) and the control inputs u converge to zero. However, we will only be able to prove that r remains bounded. The main idea is to choose u and r such that (see (11.22))

$$\dot{v} + z_2 = v - (u + z_1) r \triangleq -(v + z_2) \quad (11.28)$$

We propose the candidate Lyapunov function

$$V_3 = \frac{1}{2} (z_1^2 + z_2^2) + \frac{1}{4} (v + z_2)^2 \quad (11.29)$$

Differentiating (11.29) and using (11.28), it follows that (see (11.22))

$$\begin{aligned} \dot{V}_3 &= z_1 u + z_2 v - \frac{1}{2} (v + z_2)^2 \\ &= z_1 u - \frac{v^2}{2} - \frac{z_2^2}{2} \end{aligned} \quad (11.30)$$

Considering the following control inputs u and r

$$u = -z_1 + \sqrt{\frac{v^2}{4} + \frac{z_2^2}} \quad (11.31)$$

and

$$r = \frac{4v + 2z_2}{\sqrt{v^2 + z_2^2}} \quad (11.32)$$

The time derivative of V_3 becomes

$$\dot{V}_3 = -z_1^2 - \frac{1}{2} v^2 - \frac{z_2^2}{2} + z_1 \sqrt{\frac{v^2}{4} + \frac{z_2^2}} \sqrt{\frac{v^2}{4} + \frac{z_2^2}}$$

and by completion of squares, we get

$$\dot{V}_3 \leq -\frac{3}{4} z_1^2 - \frac{1}{4} v^2 - \frac{1}{4} z_2^2 \quad (11.33)$$

Since V_3 and $-\dot{V}_3$ are both positive definite and since

$$\frac{1}{2} (z_1^2 + v^2 + z_2^2) \leq \frac{1}{2} z_1^2 + \frac{1}{8} v^2 + \frac{1}{4} z_2^2 \leq V_3$$

and

$$V_3 \leq \frac{1}{2}z_1^2 + z_2^2 + \frac{1}{2}v^2 \leq z_1^2 + z_2^2 + v^2$$

we have thus proved that the origin of the system (11.22) is globally and exponentially stable. Moreover, u converges to zero and r is bounded ($|r| \leq 6$).

11.4.3 Third approach

We will now propose a last alternative control scheme for controlling the position of the hovercraft. This latter approach is based on the main idea (11.28) and on the candidate Lyapunov function V_3 (11.29), which we will call V_4 . The advantage of the control strategy presented here is that the state (z_1, z_2, v) converges exponentially to zero, whereas the convergence is only asymptotic in Section 11.4.1. Moreover, both control inputs u and r converge to zero.

Since $\dot{v} + z_2 \triangleq -(v + z_2)$ persists, the time derivative of V_4 remains (see (11.30))

$$\begin{aligned}\dot{V}_4 &= z_1 u + z_2 v - \frac{1}{2}(v + z_2)^2 \\ &= z_1 u - \frac{v^2}{2} - \frac{z_2^2}{2}\end{aligned}\tag{11.34}$$

We propose

$$u = -z_1 - \text{sign}(z_1)\sqrt{|2v + z_2|}\tag{11.35}$$

and

$$r = -\text{sign}(z_1(2v + z_2))\sqrt{|2v + z_2|}\tag{11.36}$$

The time derivative of V_4 becomes

$$\dot{V}_4 = -z_1^2 - |z_1|\sqrt{|2v + z_2|} - \frac{1}{2}v^2 - \frac{z_2^2}{2}\tag{11.37}$$

By completion of squares (as in Section 11.4.2), it is easy to show that this implies that the origin of the system (11.22) is globally and exponentially stable. Furthermore, u and r converge to zero.

11.5 Simulation results

In order to observe the results of the different proposed control laws, we performed simulations.

Figure 11.3 shows the results for the stabilization of the system (11.18), using the control law in (11.19) and (11.20), with $k_u = 1$ and $k_r = 1$. The initial velocities are $u(0) = 10$, $v(0) = 10$ and $r(0) = 1$. Figure 11.4 shows the simulations for the stabilization of the position of

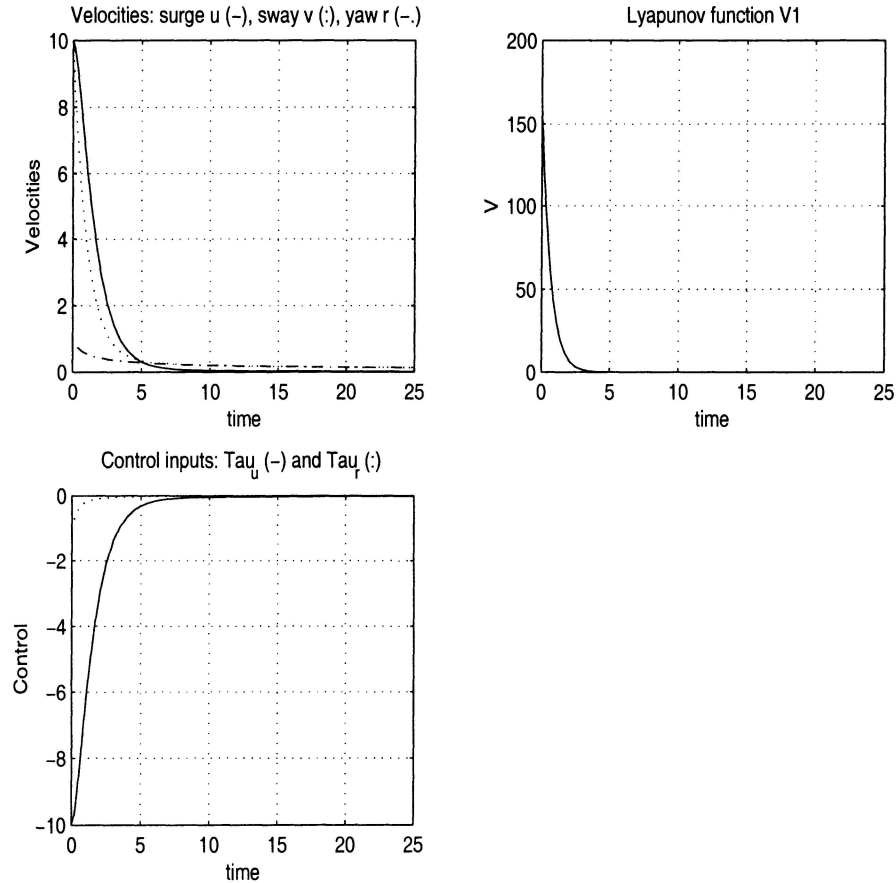


Figure 11.3: Control of the velocity using the algorithm in Section 11.3.

system (11.22) with the control law in (11.24)-(11.26). The initial positions are $z_1(0) = 0.1$, $z_2(0) = 0.1$ and $v(0) = 0$. Figure 11.5 shows the results of the control law in (11.31)-(11.32) for system (11.22), with ini-

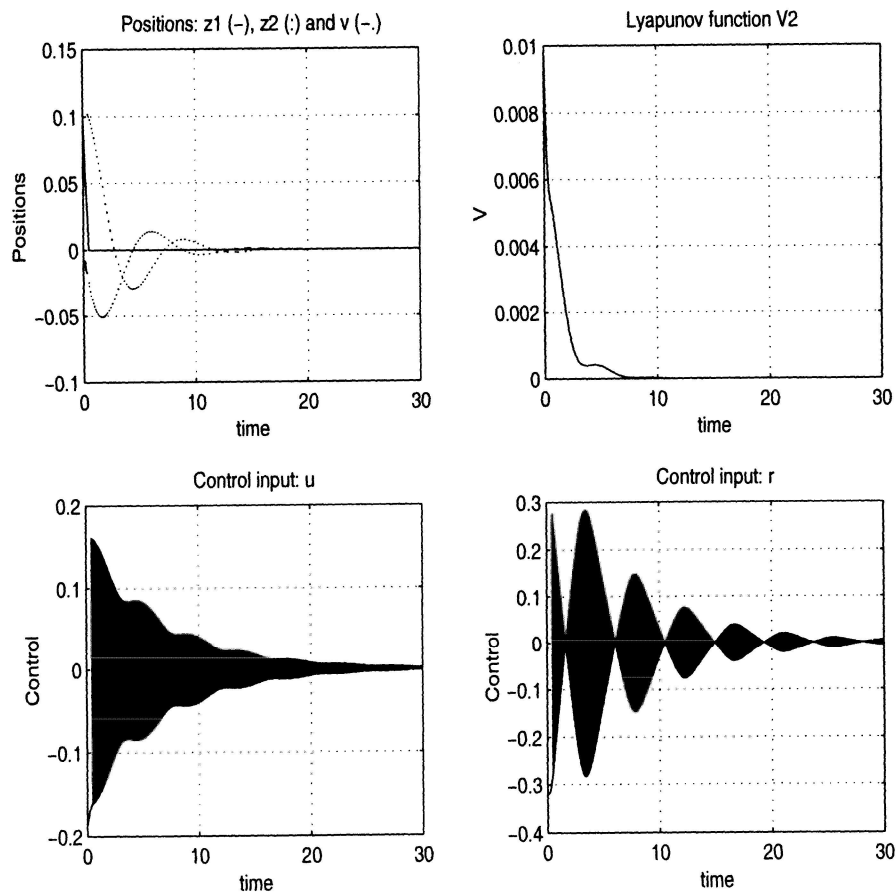


Figure 11.4: Stabilization of the position using the algorithm in Section 11.4.1: controller (11.24)-(11.26)

tial positions $z_1(0) = 10$, $z_2(0) = 10$ and $v(0) = 1$. We can choose larger initial positions, because the control does not saturate since the control law is smoother than those using the sign-function. Finally, Figure

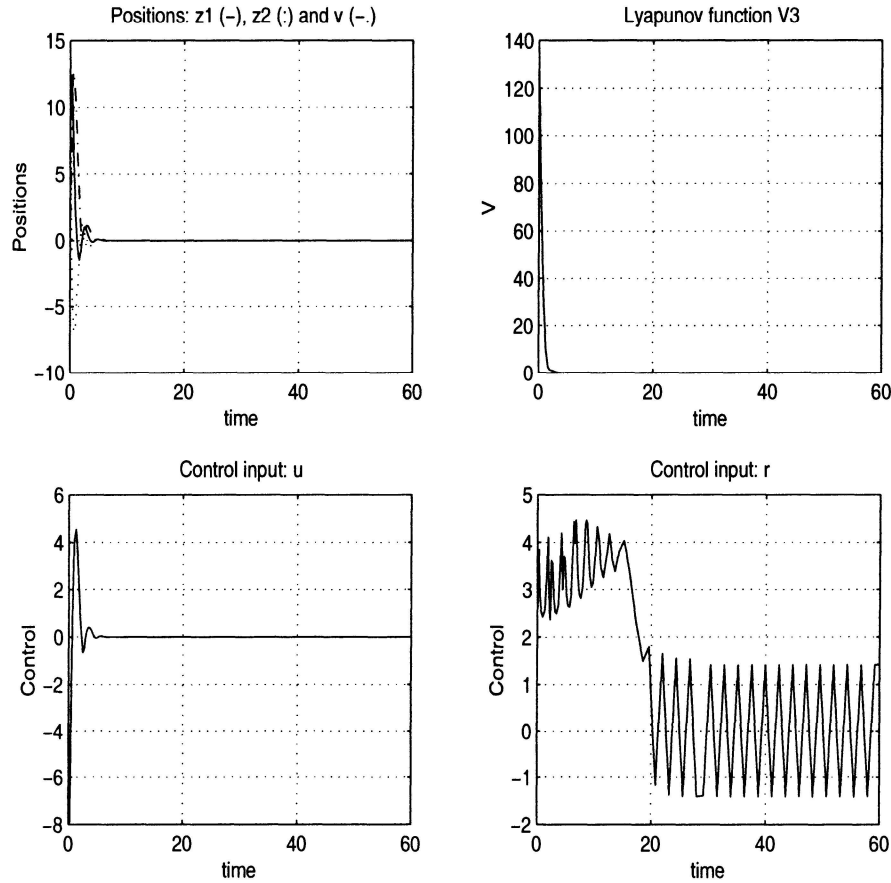


Figure 11.5: Stabilization of the position using the algorithm in Section 11.4.2: controller (11.31)-(11.32)

11.6 shows the results of the control law in (11.35)-(11.36) for system (11.22), with initial positions $z_1(0) = 0.1$, $z_2(0) = 0.1$ and $v(0) = 0$.

11.6 Conclusions

We have presented a model of an underactuated hovercraft with three degrees of freedom and two control inputs. We have proposed a control

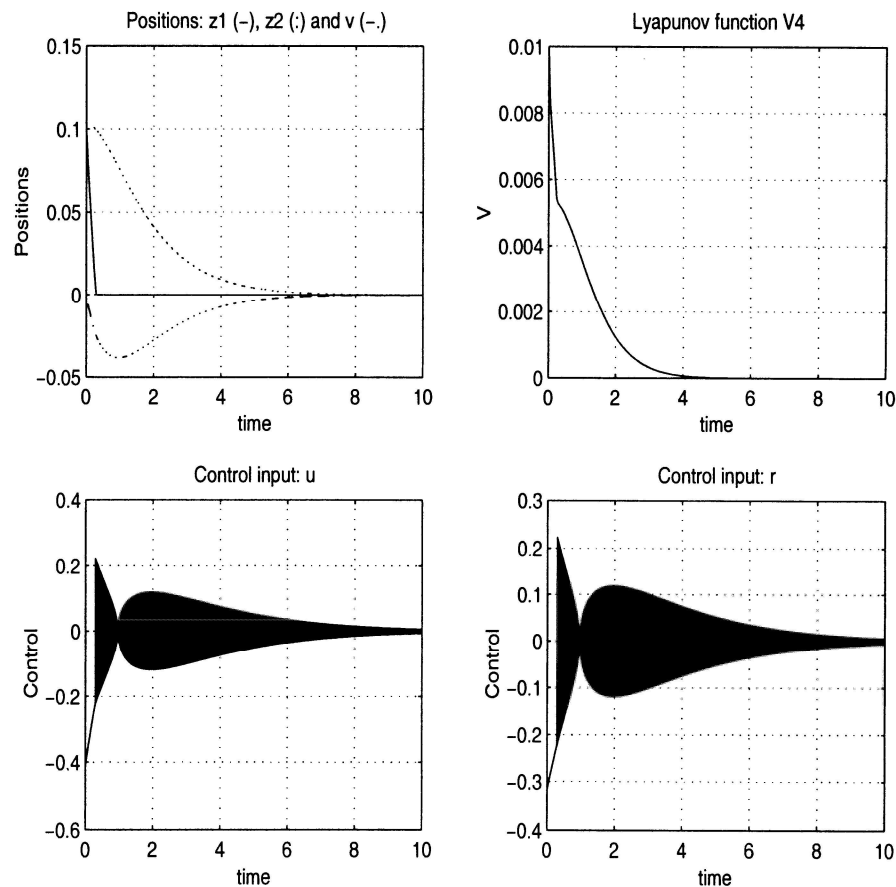


Figure 11.6: Control of the velocity using the algorithm in Section 11.4.3: (11.35)-(11.36)

scheme based on a Lyapunov approach to stabilize the surge, sway and angular velocities. We have also proposed three control strategies for positioning the vehicle using the surge and the angular velocity as virtual inputs. The three positioning controllers are discontinuous. One of the controllers is such that the origin is globally and asymptotically stable and the two inputs converge to zero. The second controller is such that the origin is globally and exponentially stable and one of the inputs (u) converges to zero while the other (r) is only proved to be bounded. The third controller is such that the origin is globally and exponentially stable and both inputs (u) and (r) converge to zero. The proposed control presents an undesired chattering behavior. Further studies are underway to better understand the control of the underactuated hovercraft model presented in this chapter. Modifications are still required to reduce the high frequency oscillations observed in simulations in order to render the controller applicable to a real system.